Lecture 3: quasi-PDF and gluon spin

A Euclidean quasi-distribution

- Consider space correlation in a large momentum P in the z-direction.

$$\tilde{q}(x,\mu^2,P^z) = \int \frac{dz}{4\pi} e^{izk^z} \langle P|\overline{\psi}(z)\gamma^z \times \exp\left(-ig\int_0^z dz' A^z(z')\right)\psi(0)|P\rangle$$

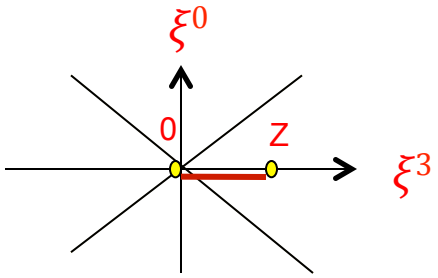

  - Quark fields separated along the z-direction
  - The gauge-link along the z-direction
  - The matrix element depends on the momentum P
  - One can use γ^4 as well instead of γ^z

Taking the limit P-> ∞ first

- After renormalizing all the UV divergences, one has the standard quark distribution!
  - One can prove this using the standard OPE
  - One can also see this by writing

    $|P\rangle = U(\Lambda(p)) \, |p=0\rangle$
  - and applying the boost operator on the gauge link.

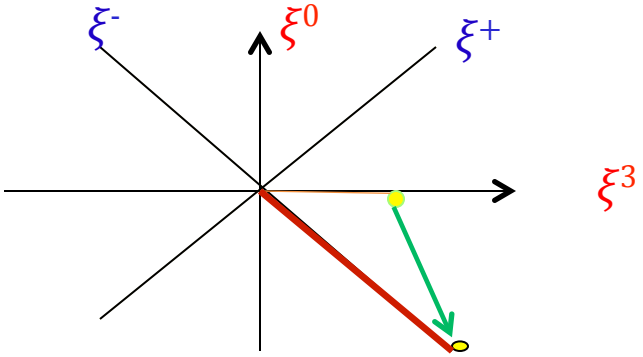

Working at finite P

- The quasi-PDFs will have log dependence on the momentum of the nucleon.
- Meanwhile, the parton density has support outside of $0<x<1$.
- However, it is closer to the physical reality because in high-energy scattering, the hadron does have FINITE momentum, and a parton could have more momentum than the parent.

Finite but large P

- The distribution at a finite but large P shall be calculable in lattice QCD.
- Since it differs from the standard PDF by simply an infinite P limit, it shall have the same infrared (collinear) physics.
- It shall be related to the standard PDF by a matching factor $Z(\mu/P)$ which is perturbatively calculable.

One-loop matching

FIG. 1: One loop corrections to quasi quark distribution.

$$\tilde{q}(x,\mu^z,P^z) = (1+\tilde{Z}_F^{(1)}+\dots)\delta(x-1)+\tilde{q}^{(1)}(x)+\dots \qquad (1)$$

with

$$\tilde{q}^{(1)}(x) = \frac{\alpha_S C_F}{2\pi}\begin{cases} \frac{1+x^2}{1-x}\ln\frac{x(\Lambda(x)-xP^z)}{(x-1)(\Lambda(1-x)+P^z(1-x))}+1-\frac{xP^z}{\Lambda(x)}+\frac{x\Lambda(1-x)+(1-x)\Lambda(x)}{(1-x)^2P^z}\,, & x>1\,, \\ \frac{1+x^2}{1-x}\ln\frac{(P^z)^2}{m^2}+\frac{1+x^2}{1-x}\ln\frac{4x(\Lambda(x)-xP^z)}{(1-x)(\Lambda(1-x)+(1-x)P^z)}-\frac{4x}{1-x}+1-\frac{xP^z}{\Lambda(x)} & \\ \quad +\frac{x\Lambda(1-x)+(1-x)\Lambda(x)}{(1-x)^2P^z}\,, & 0<x<1 \\ \frac{1+x^2}{1-x}\ln\frac{(x-1)(\Lambda(x)-xP^z)}{x(\Lambda(1-x)+(1-x)P^z)}-1-\frac{xP^z}{\Lambda(x)}+\frac{x\Lambda(1-x)+(1-x)\Lambda(x)}{(1-x)^2P^z}\,, & x<0 \end{cases} \qquad (2)$$

$$\Lambda(x) = \sqrt{\mu^2+x^2(P^z)^2}$$

Properties

- It was done in cut-off regulator so that the result will be similar for lattice perturbation theory.
- It does not vanish outside 0<x<1, because there are backward moving particles.
- All soft divergences cancels. All collinear divergences appear in 0<x<1, exactly same as the light-cone distribution.
- As $p \to \infty$ first, one recover the standard LC distribution.

Factorization or matching at one-loop

- Since the IR behavior of the quasi-distribution is the same as the LC one, one can write down easily a factorization to one-loop order.

$$\tilde{q}(x,\mu^2,P^z)=\int_{-1}^{1}\frac{dy}{|y|}Z\left(\frac{x}{y},\frac{\mu}{Pz}\right)q(y,\mu^2)+\mathcal{O}\left(\Lambda^2/(P^z)^2,M^2/(P^z)^2\right)$$

$$Z(x,\mu/P^z)=\delta(x-1)+\frac{\alpha_s}{2\pi}Z^{(1)}(x,\mu/P^z)+...$$

- Where the matching factor is perturbative.

All order proof (Qiu and Ma)

- Consider $A^3 = 0$ gauge (no subtle spurious singularity in this case).
- There are no soft-singularities in the quasi-distribution.
- All collinear singularities are in ladder diagrams, happen when P large and gluons are collinear with the P. This singularity is the same as that of the light-distribution.

Quark PDF

- For isospin non-singlet distributions, calculations are easier on lattice.
- One can calculate the quasi-distributions at finite P and match it to light-cone ones
- Several groups:
  - LP3 collaboration (MSU,MIT,…)
  - ETMC (DESY, Cypres, …)
  - Jeffferson lab group, US
  - Regensburg group, Germany
  - …

ETMC calculation (DESY, Germany)

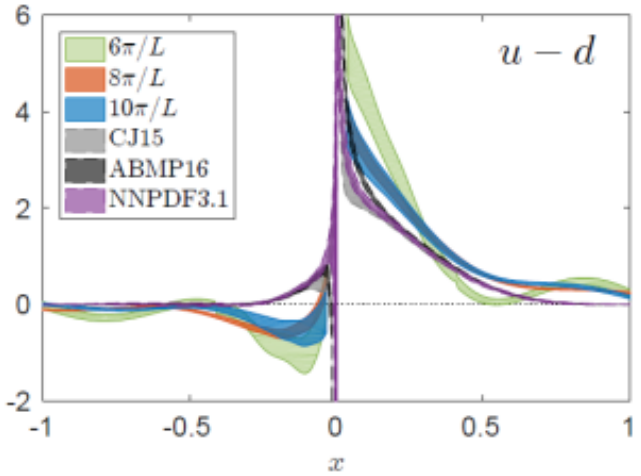

FIG. 4: Comparison of unpolarized PDF at momenta $\frac{6\pi}{L}$ (green band), $\frac{8\pi}{L}$ (orange band), $\frac{10\pi}{L}$ (blue band), and ABMP16 [39] (NNLO), NNPDF [40] (NNLO) and CJ15 [38] (NLO) phenomenological curves.

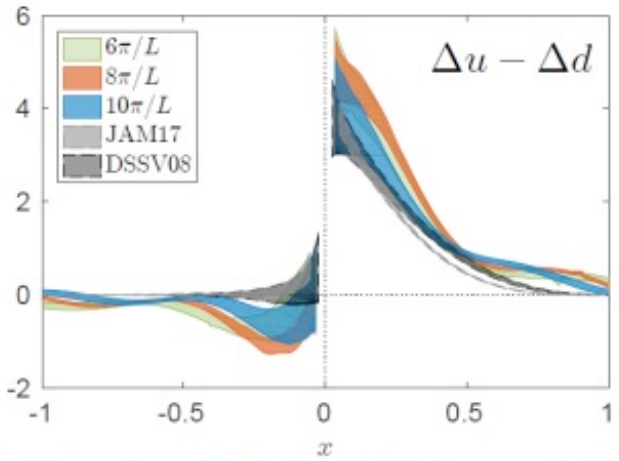

FIG. 5: Comparison of polarized PDF at momenta $\frac{6\pi}{L}$ (green band), $\frac{8\pi}{L}$ (orange band), $\frac{10\pi}{L}$ (blue band), DSSV08 [41] and JAM17 NLO phenomenological data [42].

Reconstruction of light-cone parton distribution functions from lattice QCD simulations at the physical point

Constantia Alexandrou,[1,2] Krzysztof Cichy,[3] Martha Constantinou,[4]
Karl Jansen,[5] Aurora Scapellato,[1,6] and Fernanda Steffens[7]

[1] *Computation-based Science and Technology Research Center, The Cyprus Institute, 20 Kavafi Street, Nicosia 2121, Cyprus*
[2] *Department of Physics, University of Cyprus, P.O. Box 20537, 1678 Nicosia, Cyprus*
[3] *Faculty of Physics, Adam Mickiewicz University, Umultowska 85, 61-614 Poznań, Poland*
[4] *Department of Physics, Temple University, Philadelphia, PA 19122 - 1801, USA*
[5] *NIC, DESY, Platanenallee 6, D-15738 Zeuthen, Germany*
[6] *University of Wuppertal, Gaußstr. 20, 42119 Wuppertal, Germany*
stitut für Strahlen- und Kernphysik, Rheinische Friedrich-Wilhelms-Universität Bonn, Nussallee 14-16, 5311

We present the unpolarized and helicity parton distribution functions calculated within lattice QCD simulations using physical values of the light quark mass. Non-perturbative renormalization is employed and the lattice data are converted to the $\overline{\text{MS}}$-scheme at a scale of 2 GeV. A matching process is applied together with target mass corrections leading to the reconstruction of light-cone parton distribution functions. For both cases we find a similar behavior between the lattice and phenomenological data, and for the polarized PDF a nice overlap for a range of Bjorken-x values. This presents a major success for the emerging field of direct calculations of quark distributions using lattice QCD.

LP3 Lattice Calculation

- Lattice space $a = 0.09$ fm
- Box size $64^3 \times 96$ $(L = 5.8 \text{ fm})$
- $m_\pi = 135$ MeV ($m_\pi L \approx 4.0$)
- clover valence fermions
- gauge configurations with $N_f = 2+1+1$ HISQ [1] generated by MILC Collaboration [2]
- The gauge links are hypercubic (HYP)-smeared [3]
- The quark field is Gaussian momentum smeared [4]

[1] E. Follana, Q. Mason, C. Davies, K. Hornbostel, G. P. Lepage, J. Shigemitsu, H. Trottier, and K. Wong (HPQCD, UKQCD), Phys. Rev. D75, 054502 (2007), arXiv:hep-lat/0610092 [hep-lat].

[2] A. Bazavov et al. (MILC), Phys. Rev. D87, 054505 (2013), arXiv:1212.4768 [hep-lat].

[3] A. Hasenfratz and F. Knechtli, Phys. Rev. D64, 034504 (2001), arXiv:hep-lat/0103029 [hep-lat].

[4] G. S. Bali, B. Lang, B. U. Musch, and A. Schfer, Phys. Rev. D93, 094515 (2016), arXiv:1602.05525.

Lattice Calculation

- The nucleon momentum $P\uparrow z = \{2.2, 2.6, 3.0\}$ GeV
- 884 gauge configurations
- measure the proton matrix elements with six source-sink separations {0.54, 0.72, 0.81, 0.90, 0.99, 1.08} fm with the number of {16, 32, 32, 64, 64, 128}k measurements, respectively

LP3 Collaboration, Phys. Rev. Lett. **121**, 242003 （2018）

Some details

$$\Delta\tilde{q}(x, P_z, a) = \int_{-\infty}^{\infty} \frac{P_z dz}{2\pi}\, e^{ixP_z z} \frac{1}{2P_0} \langle PS|\hat{O}(z,a)|PS\rangle$$

$\hat{O}(z,a)$ has both power and logarithmic divergences as $a \to 0$, and for the isovector combination, all divergences have been shown to factorize [17–19]. To achieve high precision in matching, a NPR for the lattice operators is used to define the continuum limit of the quasi-PDF matrix elements. Following the RI/MOM scheme advocated in Refs. [20, 27], we introduce a z-dependent renormalization factor $Z(z, p_z^R, \mu_R, a)$ defined on the lattice in an off-shell quark state in Landau gauge with z-component momentum p_z^R and subtraction scale μ_R. The renormalized matrix element of $\tilde{h}(z, P_z, a) = (1/2P_0)\langle PS|\hat{O}(z,a)|PS\rangle$ in coordinate space,

$$\tilde{h}_R(z, P_z, p_z^R, \mu_R) = Z^{-1}(z, p_z^R, \mu_R, a)\tilde{h}(z, P_z, a), \quad (2)$$

has a well defined continuum limit as $a \to 0$.

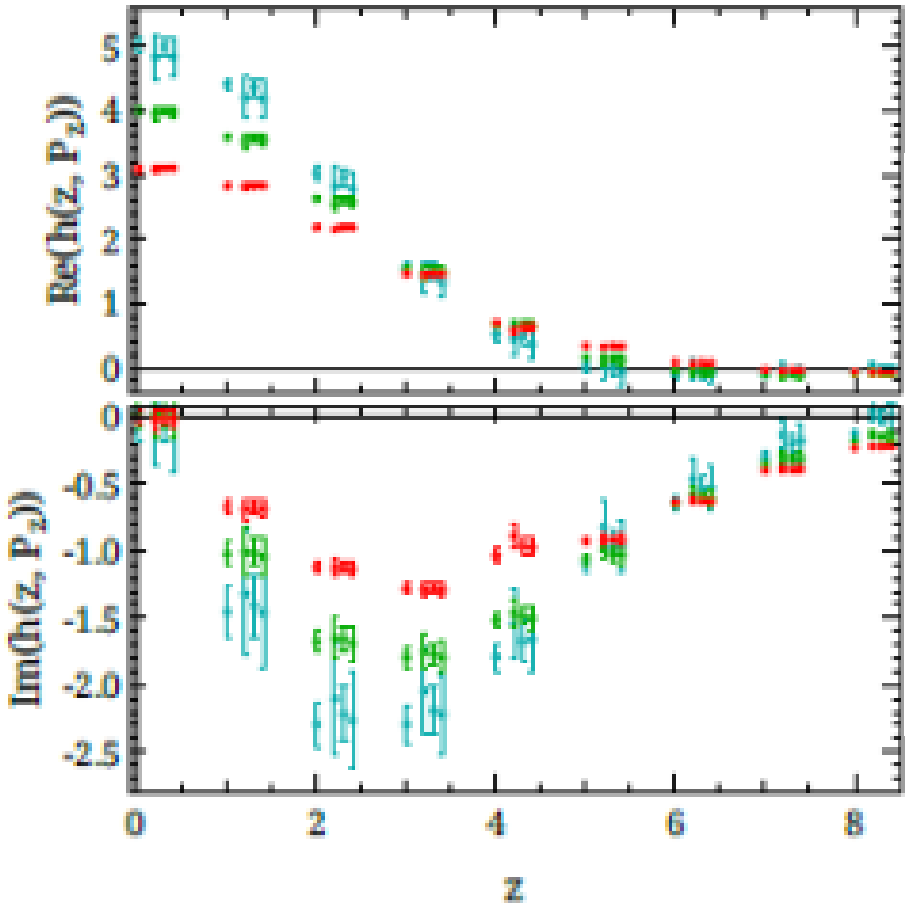

FIG. 1. The real (top) and imaginary (bottom) parts of the bare proton matrix elements for the isovector quark helicity as functions of z at all three momenta (2.2, and 2.6 and 3.0 GeV indicated by red, green and blue, respectively). Their kinematic factors have been omitted to enhance visibility by separating the small-z matrix elements. At a given positive z value, the data are slightly offset to show different ground-state extraction strategies; from left to right they are: two-simRR using all t_{sep} (Fit-1), two-simRR using the largest 5 t_{sep} (Fit-2), two-sim using the largest 4 t_{sep} (Fit-3), and two-sim using the largest 3 t_{sep} (Fit-4). All fits yield consistent results, as would be expected if the excited-state contamination is well-described by the two-state model.

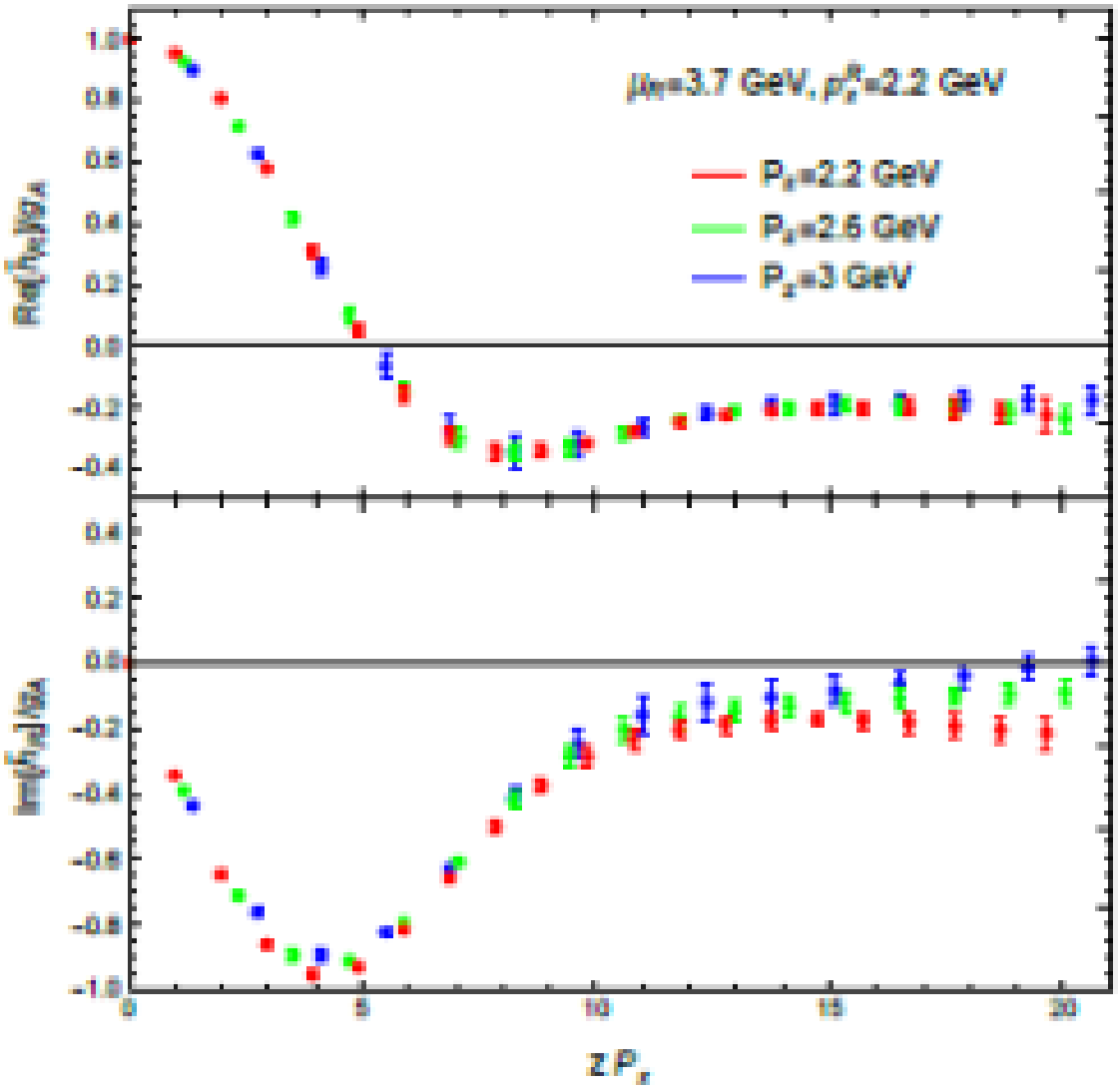

FIG. 2. The real (top) and imaginary (bottom) parts of the renormalized proton matrix elements as functions of zP_z, at renormalization scale $\mu_R = 3.7$ GeV, and $p_z^R = 2.2$ GeV.

Following the framework described in Refs. [27, 28], the matching between the renormalized quasi-PDF $\Delta\tilde{q}_R(x, P_z, p_z^R, \mu_R)$ and the physical PDF $\Delta q(y, \mu)$ at scale μ is

$$\Delta\tilde{q}_R(x, P_z, p_z^R, \mu_R) = \int_{-1}^{1} \frac{dy}{|y|} C\left(\frac{x}{y}, r, \frac{yP_z}{\mu}, \frac{yP_z}{p_z^R}\right) \Delta q(y, \mu) + \mathcal{O}\left(\frac{M^2}{P_z^2}, \frac{\Lambda_{\rm QCD}^2}{P_z^2}\right), \quad (3)$$

where $r = {\mu_R}^2/(p_z^R)^2$, M is the proton mass, and the antiquark distribution $\Delta\overline{q}(y, \mu) \equiv \Delta q(-y, \mu)$ falls in the region $-1 < y < 0$. The matching coefficient C at one-loop level using minimal projection in the $\overline{\rm MS}$ scheme can be found in Ref. [12].

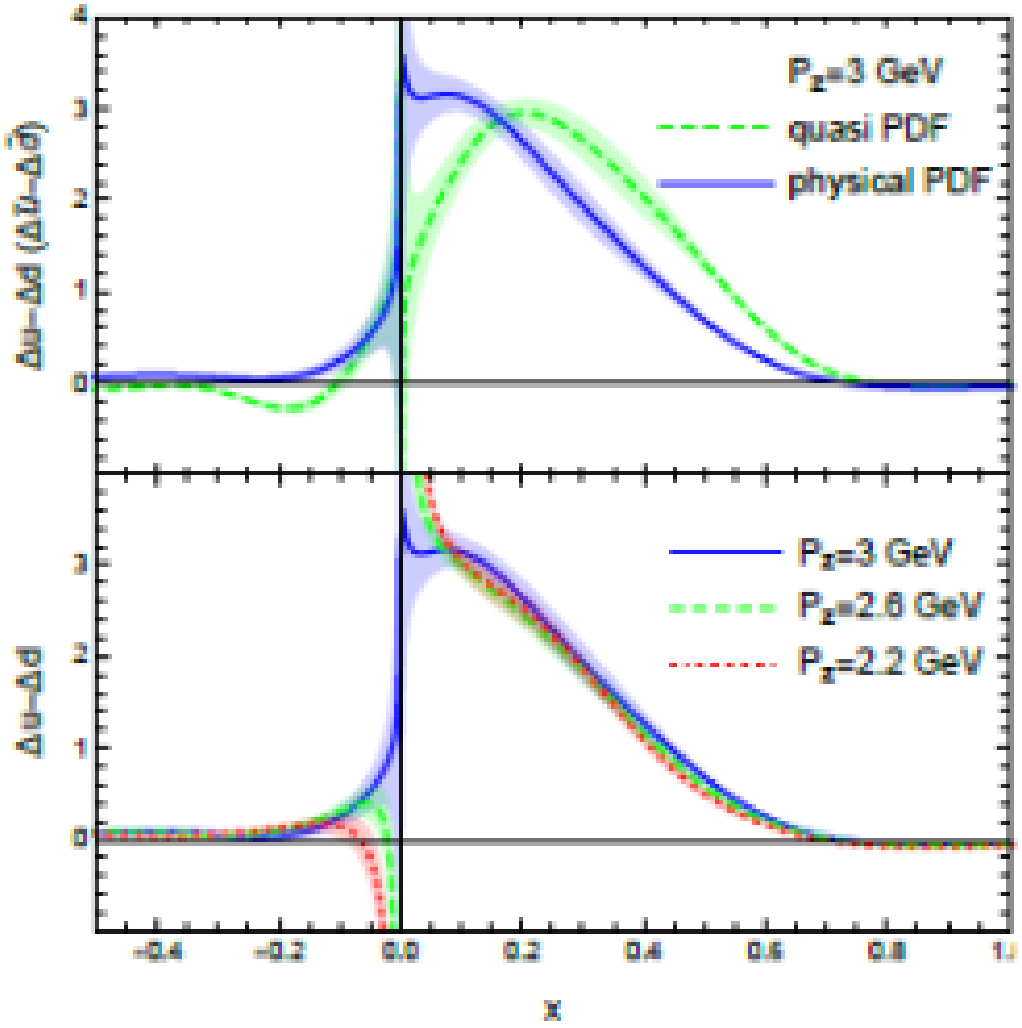

FIG. 3. The top panel is a quark helicity quasi-PDF in RI/MOM scheme at proton momentum 3.0 GeV and resulting physical PDF in $\overline{\text{MS}}$ at $\mu = 3$ GeV. The error bands are statistical. The bottom panel shows the matched physical PDFs from various proton momenta.

isovector helicity PDF [1]

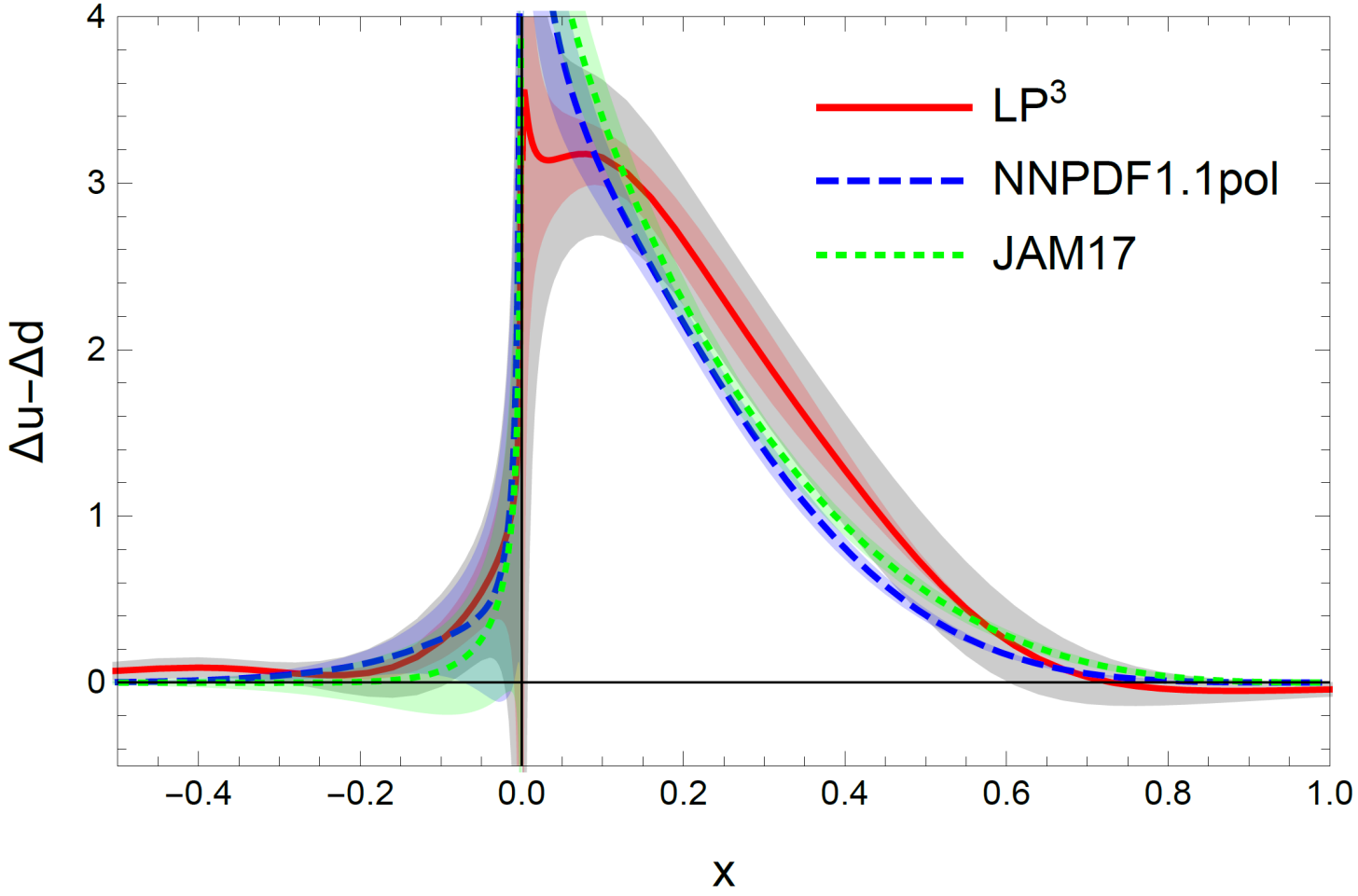

[1] H. W. Lin, J. W. Chen, X. Ji, L. Jin, R. Li, Y. S. Liu, Y. B. Yang, J. H. Zhang and Y. Zhao, Phys.Rev.Lett. 121 (2018) 242003, arXiv:1810.05043 [hep-

isovector unpolarized PDF [1]

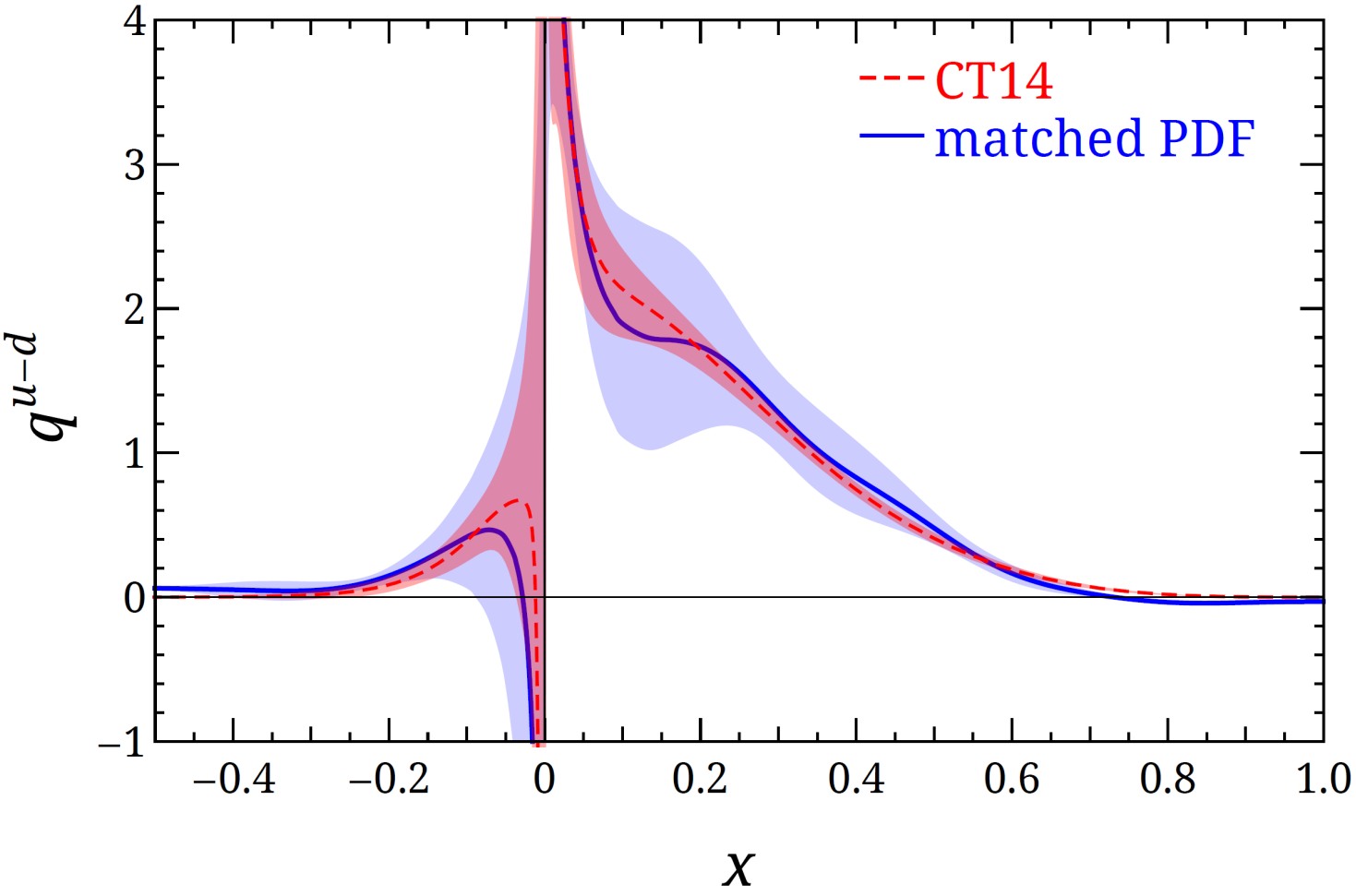

[1] J. W. Chen, L. Jin, H. W. Lin, Y. S. Liu, Y. B. Yang, J. H. Zhang and Y. Zhao, arXiv:1803.04393 [hep-lat].

isovector transversity PDF [1]

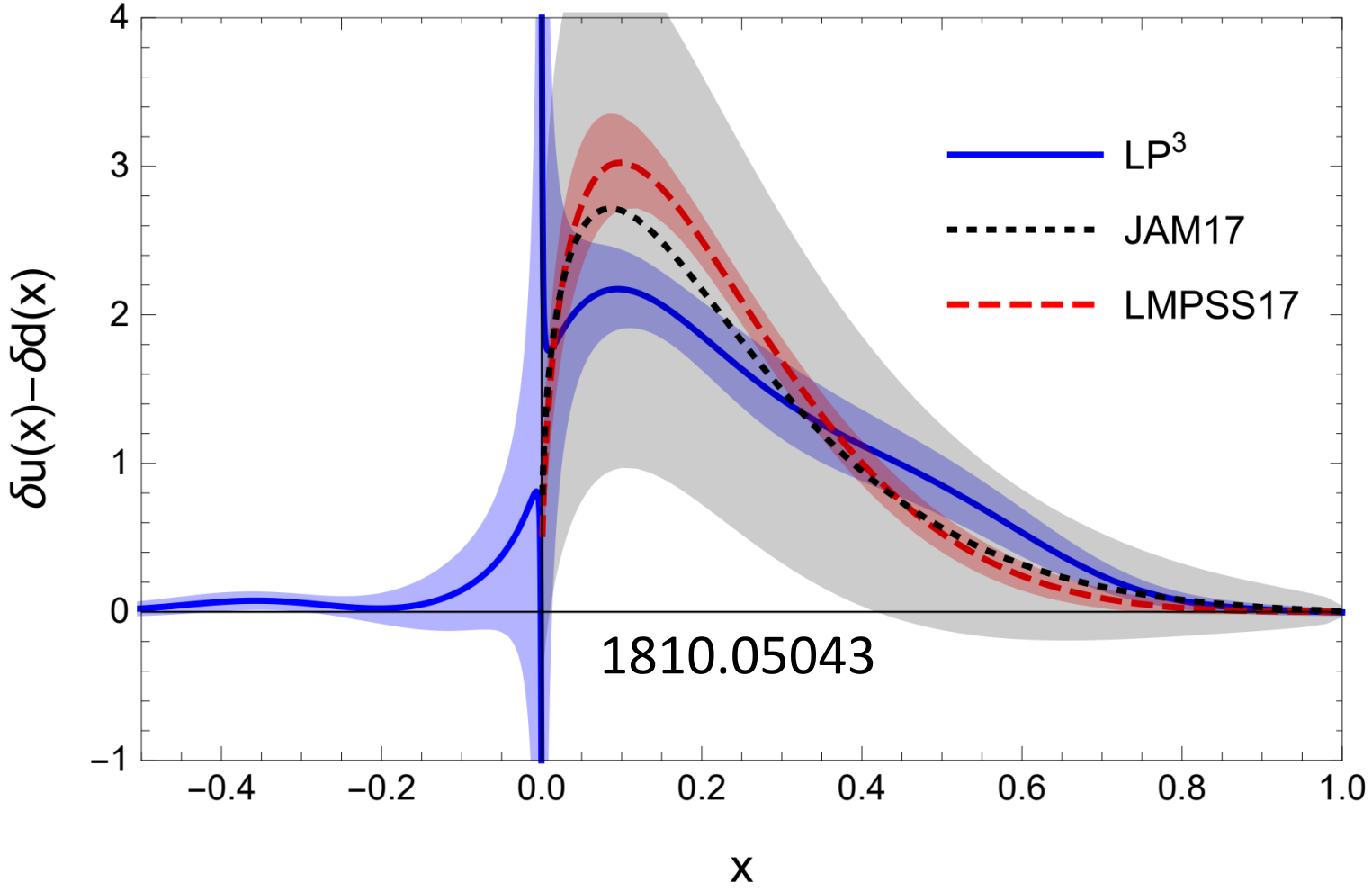

[1] Y. S. Liu, J. W. Chen, L. Jin, R. Li, H. W. Lin, Y. B. Yang, J. H. Zhang and Y. Zhao, arXiv:1810.05043 [hep-lat].

Proton spin crisis

- In the simple quark model, the proton is made of 3 quarks. The spin of the proton is entirely from the spin of unpaired quark.
- In 1987, EMC at CERN published a paper showing that only a small fraction of the proton spin comes from quark spin.
- Where is the proton spin coming from ?

"Spin crisis"

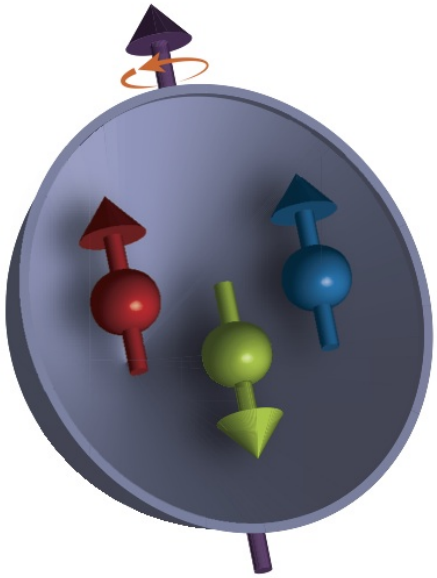

Proton spin decomposition

- For a proton with polarization along the direction of motion (helicity=1/2), the spin sum rule is

$$\tfrac{1}{2} = \tfrac{1}{2}\Delta\Sigma + \Delta G + \ell_q + \ell_g$$

ΔG: gluon helicity

$\ell_{q,g}$: orbital angular momentum of quarks and gluons

- All terms are related to parton properties, as defined in the infinite-momentum frame.

Gluon polarization ΔG

- Believed to contribute significantly to the proton spin.
- Measurable in polarized PP collision at RHIC (a physical observable)
- However, there is no gauge-invariant local operator corresponds to this quantity. (nature of gauge theory!)

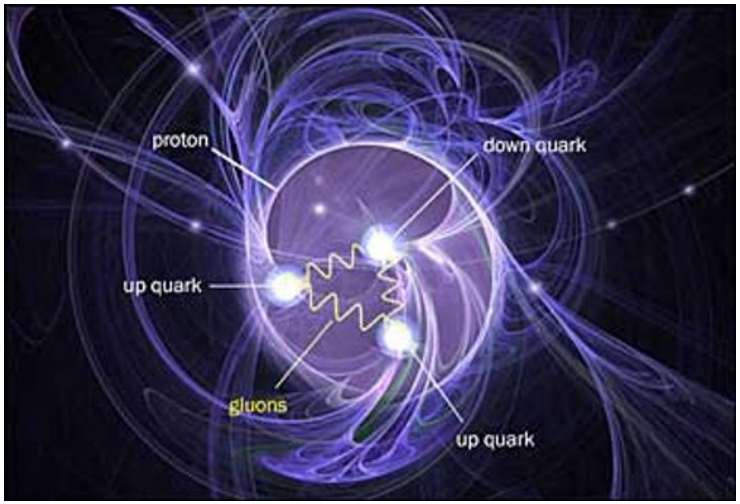

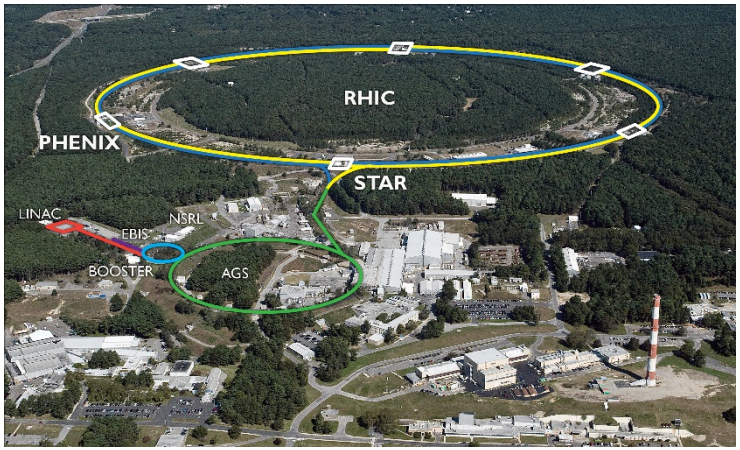

RHIC spin experiment

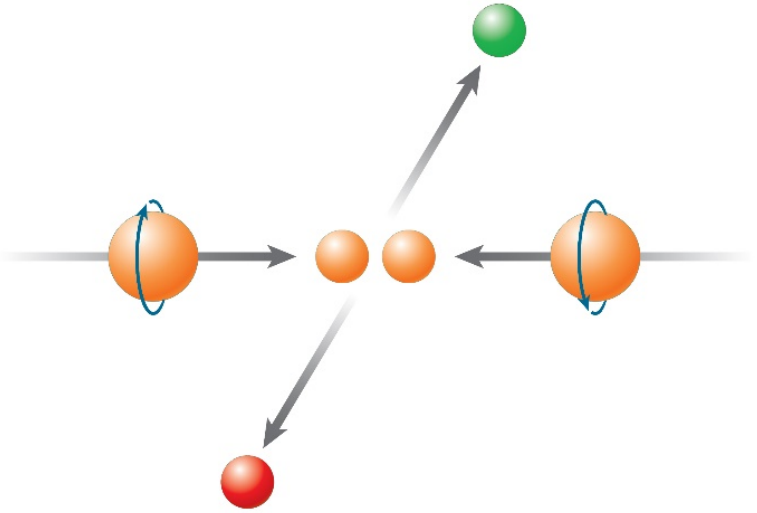

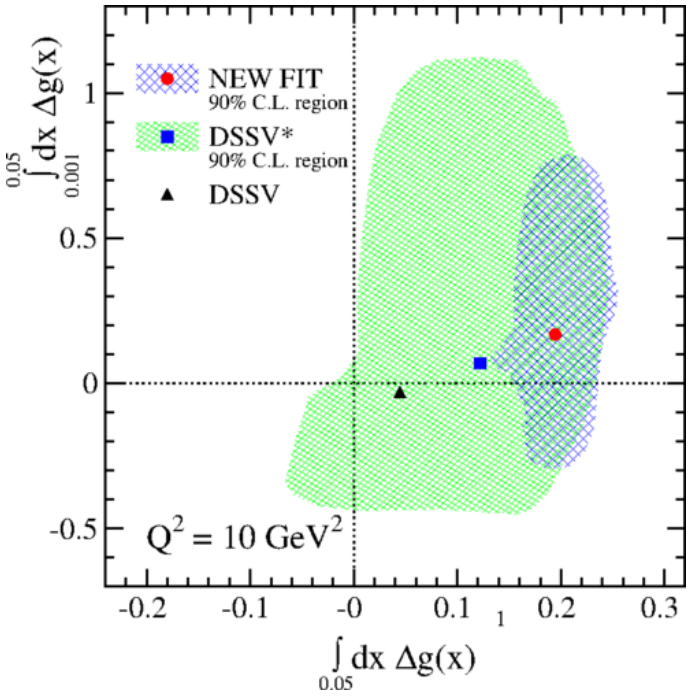

Vogelsang et al

$\Delta G \sim 0.2\hbar$

QCD factorization

- In QCD factorization, one can show that the gluon polarization is a matrix element of non-local light-cone correlations.

$$\Delta G = \int dx \frac{i}{2xP^+} \int \frac{d\xi^-}{2\pi} e^{-ixP^+\xi^-} \langle PS|F_a^{+\alpha}(\xi^-) \times \mathcal{L}^{ab}(\xi^-, 0)\tilde{F}^+_{\alpha,b}(0)|PS\rangle,$$

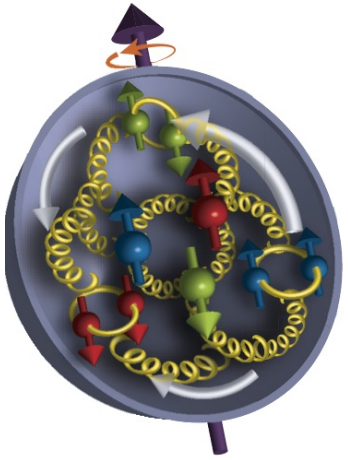

- No one knows how to calculate this for nearly 30 years!

LaMET calculations

- In LaMET theory, one can start with the local operator $\vec{E} \times \vec{A}$ in a physical gauge in the sense that the gauge condition shall allow transverse polarized gluons:
  - Coulomb gauge $\nabla \cdot E = 0$
  - Axial guage $A_z = 0$
  - Temporal gauge $A_0 = 0$
- Their matrix elements in the large momentum limit all go to ΔG.

Ji, Zhang, Zhao, Phys. Rev. Lett.,111,112002(2013)

First calculation (Yang et al, PRL (2017))

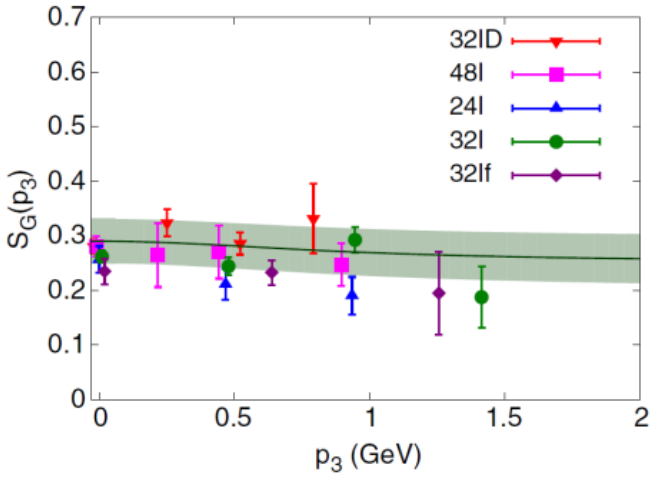

FIG. 4. The results extrapolated to the physical pion mass as a function of the absolute value of $\vec{p} = (0, 0, p_3)$, on all the five ensembles. All the results have been converted to $\overline{\text{MS}}$ at $\mu^2 = 10\ \text{GeV}^2$. The data on several ensembles are shifted horizontally to enhance the legibility. The green band shows the frame dependence of the global fit [with the empirical form in Eq. (11)] of the results.

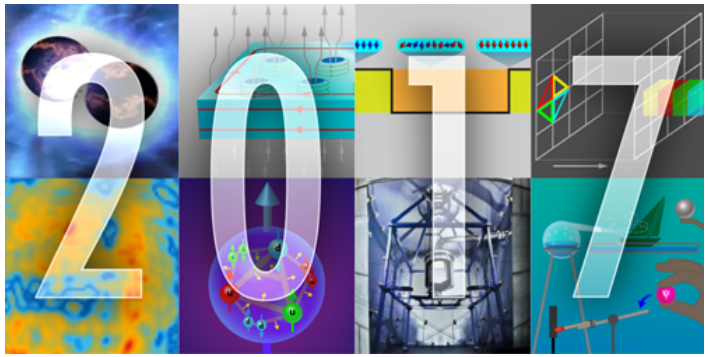

Gluons Provide Half of the Proton's Spin

The gluons that bind quarks together in nucleons provide a considerable chunk of the proton's total spin. That was the conclusion reached by Yi-Bo Yang from the University of Kentucky, Lexington, and colleagues (see Viewpoint: **Spinning Gluons in the Proton**). By running state-of-the-art computer simulations of quark-gluon dynamics on a so-called spacetime lattice, the researchers found that 50% of the

Other contributions

- QCD Angular momentum operator:

$$\vec{J} = \int d^3x\ \psi^\dagger \frac{\vec{\Sigma}}{2}\psi + \int d^3x\ \psi^\dagger \vec{x} \times (-i\vec{\nabla})\psi + \int d^3x\ \vec{E}_a \times \vec{A}^a + \int d^3x\ E^i_a\ \vec{x} \times \vec{\nabla} A^{i,a}\ ,$$

- Define quasi-observables according to

$$\frac{1}{2} = \frac{1}{2}\Delta\widetilde{\Sigma}(\mu, P^z) + \Delta\widetilde{G}(\mu, P^z) + \Delta\widetilde{L}_q(\mu, P^z) + \Delta\widetilde{L}_g(\mu, P^z)\ ,$$

LaMET Matching Formula

$$
\begin{aligned}
\Delta\widetilde{\Sigma}(\mu, P^z) &= \Delta\Sigma(\mu) \ , \\
\Delta\widetilde{G}(\mu, P^z) &= z_{qg}\Delta\Sigma(\mu) + z_{gg}\Delta G(\mu) + O\left(\frac{M^2}{(P^z)^2}\right) \ , \\
\Delta\widetilde{L}_q(\mu, P^z) &= P_{qq}\Delta L_q(\mu) + P_{gq}\Delta L_g(\mu) \\
&\quad + p_{qq}\Delta\Sigma(\mu) + p_{gq}\Delta G(\mu) + O\left(\frac{M^2}{(P^z)^2}\right) \ , \\
\Delta\widetilde{L}_g(\mu, P^z) &= P_{qg}\Delta L_q(\mu) + P_{gg}\Delta L_g(\mu) \\
&\quad + p_{qg}\Delta\Sigma(\mu) + p_{gg}\Delta G(\mu) + O\left(\frac{M^2}{(P^z)^2}\right) \ ,
\end{aligned}
$$

One-loop result for matching

$$
\begin{aligned}
z_{qg}(\mu/P^z) &= \frac{\alpha_S C_F}{4\pi}\left(\frac{4}{3}\ln\frac{(P^z)^2}{\mu^2}+R_1\right)\,, \\
z_{gg}(\mu/P^z) &= 1+\frac{\alpha_S C_A}{4\pi}\left(\frac{7}{3}\ln\frac{(P^z)^2}{\mu^2}+R_2\right)\,.
\end{aligned}
$$

$$
\begin{aligned}
P_{qq} &= 1+\frac{\alpha_S C_F}{4\pi}\left(-2\ln\frac{(P^z)^2}{\mu^2}+R_3\right) \quad , \quad P_{gq} = 0\,, \\
P_{qg} &= \frac{\alpha_S C_F}{4\pi}\left(2\ln\frac{(P^z)^2}{\mu^2}-R_3\right) \quad , \quad P_{gg} = 1\,, \\
p_{qq} &= \frac{\alpha_S C_F}{4\pi}\left(-\frac{1}{3}\ln\frac{(P^z)^2}{\mu^2}+R_4\right) \quad , \quad p_{gq} = 0\,, \\
p_{qg} &= \frac{\alpha_S C_F}{4\pi}\left(-\ln\frac{(P^z)^2}{\mu^2}-R_1-R_4\right)\,, \\
p_{gg} &= \frac{\alpha_S C_A}{4\pi}\left(-\frac{7}{3}\ln\frac{(P^z)^2}{\mu^2}-R_2\right)\,,
\end{aligned}
$$

White Paper for the Electron-Ion Collider

December 2012

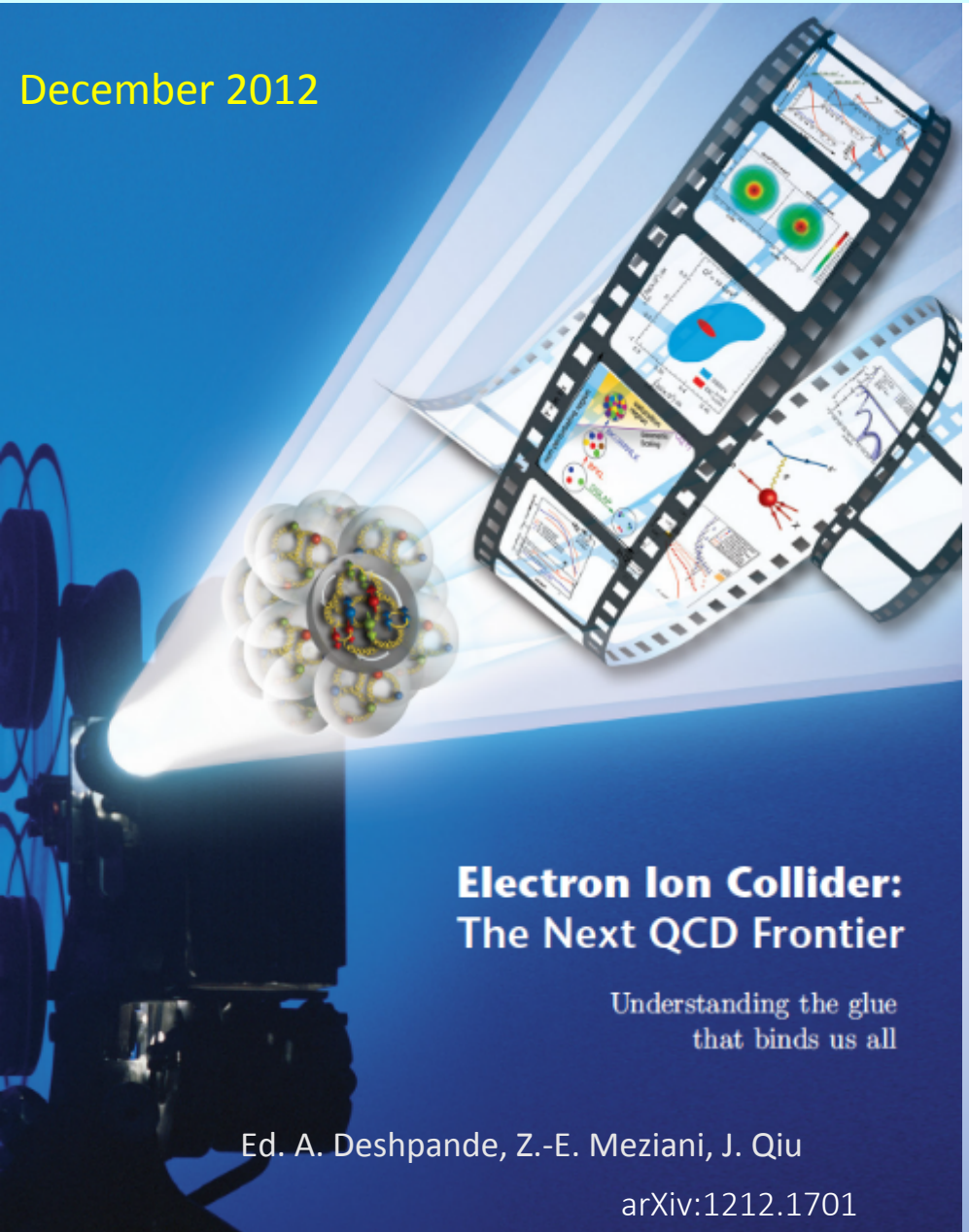

Ed. A. Deshpande, Z.-E. Meziani, J. Qiu

arXiv:1212.1701

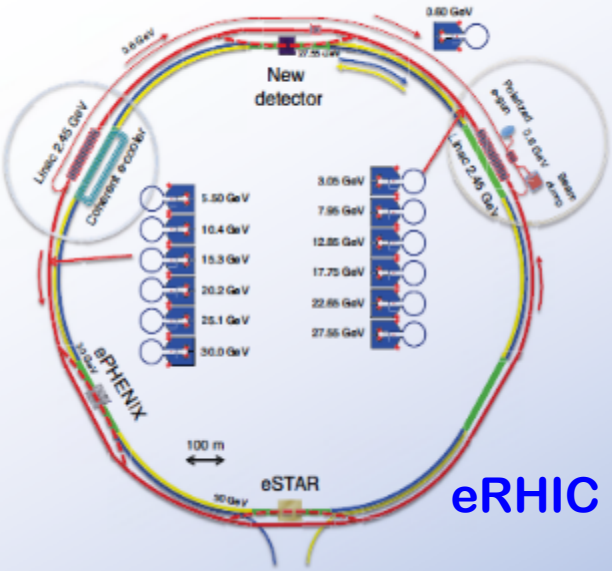

eRHIC (BNL)

ELIC (JLab)

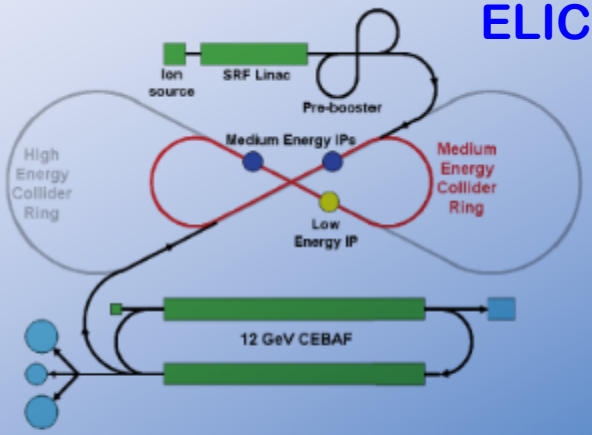

Proton tomography

- **3D boosted partonic structure:**

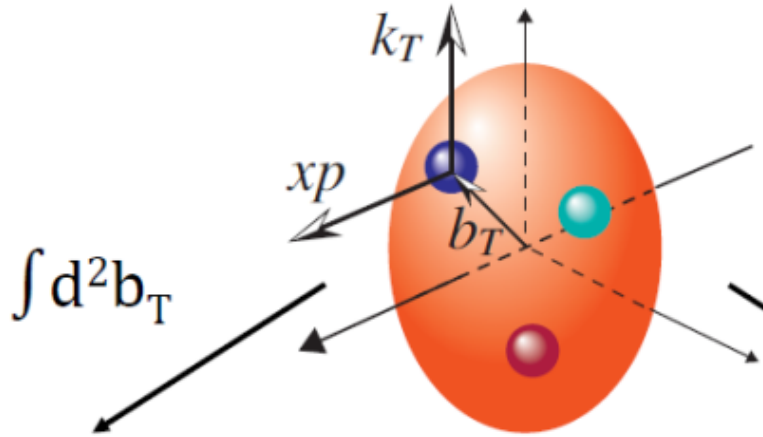

Momentum Space

TMDs

$\int d^2b_T$

$\int d^2k_T$

Coordinate Space

GPDs

$f(x,k_T)$

$f(x,b_T)$

Quarks

From EIC white paper: arXiv:1212.1701

Gluons

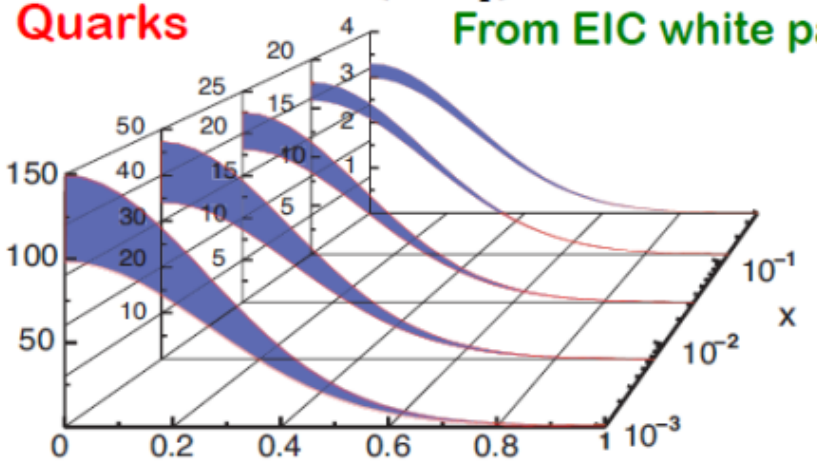

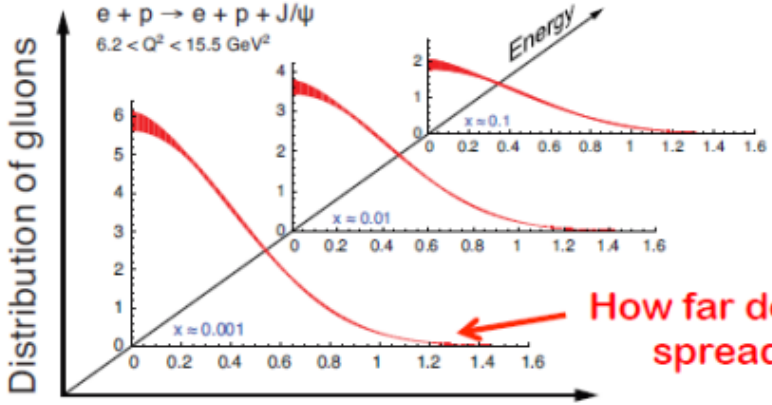

How far does it spread?

Conclusion

- All light-cone physics can be accessed through lattice QCD in large momentum effective theory
- It is just the beginning of the field, there is a lot to be done.